

Raman spectroscopy study of ferroelectric modes in [001]-oriented $0.67\text{Pb}(\text{Mg}_{1/3}\text{Nb}_{2/3})\text{O}_3\text{--}0.33\text{PbTiO}_3$ single crystals

Mingrong Shen, G. G. Siu, and Z. K. Xu

Department of Physics and Materials Science, City University of Hong Kong, Kowloon, Hong Kong, China

Wenwu Cao^{a)}

Department of Physics and Materials Science, City University of Hong Kong, Kowloon, Hong Kong, China

and Department of Mathematics and Materials Research Institute, The Pennsylvania State University, University Park, Pennsylvania 16802

(Received 14 February 2005; accepted 10 May 2005; published online 17 June 2005)

This work investigates the evolution of micro-Raman spectra of a [001]-oriented $0.67\text{Pb}(\text{Mg}_{1/3}\text{Nb}_{2/3})\text{O}_3\text{--}0.33\text{PbTiO}_3$ single crystal in the temperature range from -120 to 200 °C. For a poled sample, the T_{1u} mode splits into an E mode (remaining at 51 cm^{-1}) and a new A_1 mode (shifting to 95 cm^{-1} at -120 °C) at the tetragonal to rhombohedral phase transition ($T_c \sim 70$ °C), while other modes remain the same. This A_1 mode belongs to the rhombohedral phase. If the sample is depoled, this A_1 mode persists for temperatures much above T_c on heating, implying that local regions with rhombohedral symmetry still exist in the tetragonal phase. The underdevelopment of long-range order in the depoled crystal causes the sample to have typical characteristics of a relaxor while poling will enhance the long-range order to make it into a regular ferroelectric. © 2005 American Institute of Physics. [DOI: 10.1063/1.1948514]

Lead magnesiomniobate, $\text{Pb}(\text{Mg}_{1/3}\text{Nb}_{2/3})\text{O}_3$ (PMN), is a typical relaxor ferroelectrics which exhibits a diffuse phase transition characterized by a strong frequency dispersion of the dielectric susceptibility at temperatures near and below the T_{max} (265 K at 1 kHz). PMN has quenched chemical disorder on the perovskite B site, which is occupied by either Mg^{2+} or Nb^{5+} cations.¹ When doped with PbTiO_3 (PT), the compounds $(1-x)\text{PMN}\text{--}x\text{PT}$ (PMN-PT) exhibit a drastic increase in piezoelectric properties. The crystals with compositions near the morphotropic phase boundary (MPB) ($x = 0.33\text{--}0.34$) have piezoelectric constant $d_{33} > 2400\text{ pC/N}$, and the electromechanical coupling coefficient $k_{33} > 90\%$, when they are poled along [001] of cubic coordinates.^{2,3} The origin of this giant piezoelectricity was suggested as due to orientation effect.^{4,5}

Since the PMN-PT system is a solid solution of relaxor PMN and ferroelectric PT, there are many interesting physical phenomena in this system owing to the competition of the two. At the MPB composition, the relaxor and ferroelectric characteristics are somewhat balanced, hence, the conversion between nano-domains (relaxor nature) and macro-domains (ferroelectric nature) can be more conveniently studied in the MPB system.

Because its vibrational spectrum has a shorter characteristic length scale, Raman spectrum is a good microprobe to study the nanodomain structures that are the key for the interpretation of the relaxor properties.⁶ Previous results on both relaxor ferroelectrics and relaxor-based ferroelectrics showed that, even in the high-temperature cubic phase, the Raman spectra do not differ qualitatively from those of low symmetry phases except intensity variations of some modes. Unique ferroelectric modes have not been observed in the low symmetry phases up to date.^{6–12} There are already some studies on Raman spectra of PMN-PT crystals in the

literature.^{6,8,10,11} Here we will try to answer the question of whether the tetragonal to rhombohedral structural change has any corresponding changes in the vibrational spectrum. In this work, micro-Raman measurements were performed on a [001] oriented $0.67\text{PMN}\text{--}0.33\text{PT}$ single crystal, which could provide interesting information about the phase transition from tetragonal to rhombohedral phase since the composition is near the MPB. Most importantly, we have found a unique mode splitting that can signify this phase transition.

The single crystal used in this study is transparent with light-yellow color. It is [001] oriented with the composition of $0.67\text{Pb}(\text{Mg}_{1/3}\text{Nb}_{2/3})\text{O}_3\text{--}0.33\text{PbTiO}_3$. The crystal was cut into a plate and optically polished. The dimensions of the plate are 3 mm on each side and 0.7 mm in thickness. Before the Raman measurements, the crystal was annealed at 300 °C for half an hour in air to remove possible residual stresses and polarization. Micro-Raman scattering spectra were recorded in back scattering geometry using a JY T64000 micro-Raman spectrometer with a coherent Ar ion laser. The excitation line is at 514.5 nm and the light spot size is about $1\text{ }\mu\text{m}$ using the $\times 100$ objective lens. The spectra were presented without polarization analysis in order to displaying all observable features.

In a recent study, temperature-dependent dielectric behavior and related phase transitions of the [001] oriented $0.67\text{PMN}\text{--}0.33\text{PT}$ crystal were investigated by impedance measurements and high resolution x-ray diffraction.¹³ It was demonstrated that a phase transition from the rhombohedral symmetry to the tetragonal symmetry occurs near 70 °C on heating, which is more clearly shown in the poled sample than in depoled sample. In the present study, we performed Raman spectroscopy study on both poled and depoled samples. Figure 1 shows the light-scattering spectra for temperatures from 180 °C down to -120 °C for the poled sample. It can be seen that all bands are relatively broad, indicating band overlapping, which is typical for perovskite relaxor-based ferroelectrics. The Raman spectra at tempera-

^{a)}Electronic mail: cao@math.psu.edu

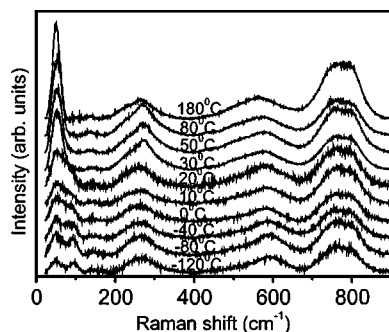


FIG. 1. Raman-scattering spectra measured in the poled [001]-oriented $0.67\text{Pb}(\text{Mg}_{1/3}\text{Nb}_{2/3})\text{O}_3-0.33\text{PbTiO}_3$ single crystal from -120 to 220 °C.

tures above 30 °C are similar to those of the $0.81\text{PMN}-0.29\text{PT}$, where four bands centered near 780 , 580 , 270 , and 51 cm^{-1} had been found.¹⁰ These four modes correspond mainly to Nb–O–Mg stretching mode, oxygen bending vibration, B-site ion against O stretching vibration inside the octahedral, and Pb against BO_6 octahedra translational vibration, respectively.¹⁴ On the one hand, the frequencies and bandwidths of the three bands centered near 780 , 580 , and 270 cm^{-1} are essentially temperature independent, similar to the results found in $0.81\text{PMN}-0.29\text{PT}$ crystals.¹² Interestingly, the Pb mode at 51 cm^{-1} shows strong temperature dependence. This mode is in fact a composite mode, which starts to bulge at 30 °C then gradually splits into two peaks upon further cooling. The new mode shifts towards higher frequency with decreasing temperature. It is at 71 cm^{-1} at 20 °C and keeps on shifting up until 95 cm^{-1} at -120 °C.

The sample was depoled by heating above 200 °C then cooling back down to room temperature without applying electric field. Raman experiments were carried out during heating from -120 to ~ 200 °C for the depoled sample and the spectrum was taken when the temperature was held at each selected temperature for 5 min. The results from -20 to 80 °C are shown in Fig. 2. The Raman spectra at temperatures lower than 0 °C are similar to those of the poled sample (Fig. 1). At -120 °C, the lowest frequency band consists of twin peaks at 51 and 96 cm^{-1} , respectively. The 96 cm^{-1} peak has the tendency to merge into the 51 cm^{-1} peak on heating, but never disappears completely like in the case of poled sample. It shifts to lower frequency on heating until 55 °C but comes back up again when the temperature rises above 60 °C. Its peak position is centered at 89 cm^{-1} at 70 °C. At higher temperatures, these two peaks are difficult to identify owing to the increasing bandwidth. As a result, the shape of the peak becomes asymmetric.

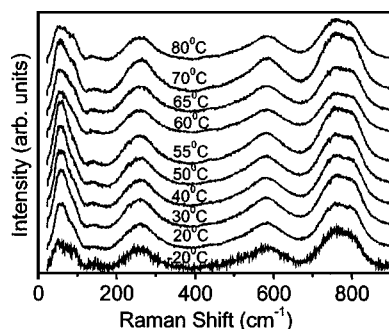


FIG. 2. Raman-scattering spectra measured in the depoled [001]-oriented $0.67\text{Pb}(\text{Mg}_{1/3}\text{Nb}_{2/3})\text{O}_3-0.33\text{PbTiO}_3$ single crystal from -120 to 220 °C.

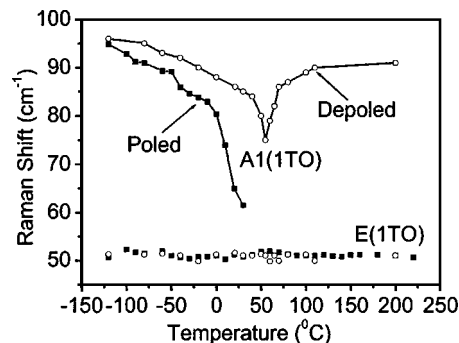


FIG. 3. Temperature dependence of the $E(1\text{TO})$ and $A_1(1\text{TO})$ modes in poled (full squares) and depoled (open circles) [001]-oriented $0.67\text{Pb}(\text{Mg}_{1/3}\text{Nb}_{2/3})\text{O}_3-0.33\text{PbTiO}_3$ single crystals.

The labeling scheme of Burns and Scott¹⁵ has been used here for clarifying the origin of the twin peaks. In the cubic perovskite paraelectric phase, there are 12 optic modes which belong to the $3T_{1u}+T_{2u}$ irreducible representation of the O_h point group. The T_{1u} modes are infrared active (IR) and the T_{2u} mode is a “silent mode” since it is neither infrared nor Raman active. In the tetragonal (C_{4v}) and rhombohedral (C_{3v}) structures of the ferroelectric phase, each triply degenerate T_{1u} mode splits into A_1 and E modes, while the T_{2u} silent mode splits into B_1 and E modes. In addition, long-range electrostatic forces in the ferroelectric phase split all the A_1+E Raman and IR active modes into LO and TO components. Thus, the $T_{1u}(\text{TO})$ mode of the paraelectric cubic phase splits into $A_1(1\text{TO})$ and $E(1\text{TO})$ modes in the lower symmetry tetragonal or rhombohedral phase. At room temperature, the 1TO modes in pure PMN and $0.81\text{PMN}-0.29\text{PT}$ crystals are centered near 55 and 79 cm^{-1} , while the 2TO modes are near 216 and 232 cm^{-1} , respectively.^{8,10} In addition, the mode below 100 cm^{-1} observed in other compositions of PMN–PT crystals and pure PMN crystal is generally assigned to the $E(1\text{TO})$ mode.^{8,10} In the present study, we attribute the modes near 51 and 95 cm^{-1} at -120 °C to $E(1\text{TO})$ and $A_1(1\text{TO})$ modes, respectively.

After fitting with a symmetric Lorentzian profile for the lowest frequency band in the Raman spectra of the poled and depoled samples, the frequency changes of these $E(1\text{TO})$ and $A_1(1\text{TO})$ modes are plotted as a function of temperature in Fig. 3. It can be seen that the frequency of the $E(1\text{TO})$ mode is almost independent of temperature from -120 to 300 °C. However, the $A_1(1\text{TO})$ does depend on temperature. For the poled sample, its frequency decreases from 95 cm^{-1} at -120 °C to 71 cm^{-1} at 20 °C, and becomes indistinguishable from the E mode above 30 °C. For the depoled sample, the $A_1(1\text{TO})$ mode also shifts towards the E mode while heating up from -120 to 55 °C, but never disappears or merges to the E mode. In fact, it grows back with further heating above 55 °C.

Previous Raman studies on relaxor and relaxor-based compounds have shown that, contrary to the group theory predictions, Raman-active vibrational modes are observable in the paraelectric phase due to the presence of low symmetry nanoclusters. This is consistent with our results. Most of the modes (such as modes near 780 , 580 , 270 , and 51 cm^{-1}) do not obviously change on heating or cooling and have no soft mode behavior near any of the structural phase transitions. The persistence of Raman peaks in the cubic phase shows that the local symmetry deviates from the overall av-

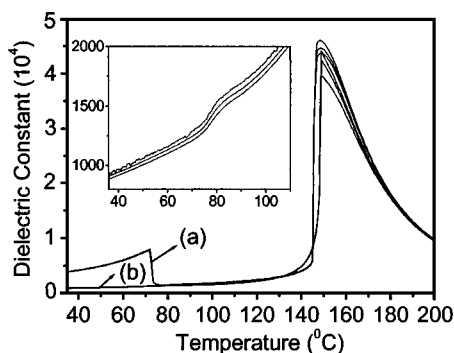


FIG. 4. Temperature dependence of the dielectric constant under different frequencies for (a) poled sample and (b) depoled sample. Each case was measured using three different frequencies: 100 Hz, 1, and 10 kHz. Relatively larger values correspond to lower frequencies. The inset is the enlarged low-temperature region of (b), where a weak shoulder occurs at the rhombohedral to tetragonal phase transition.

erage cubic structures of the relaxor compound. The relevant vanishing temperature for these Raman modes should be much higher than that of the ferroelectric transition temperature, namely should be around the Burns temperature T_d , above which the polar nanoclusters disappear completely.^{15–17}

The presence of Raman modes in the paraelectric cubic phase is generally ascribed to the presence of nanoscale chemical/structural inhomogeneities in the relaxor and relaxor-based compounds. Such inhomogeneities result in local polar clusters, or nanodomains, which have lower symmetry. The short-range order nanodomains with off-axis shift of lead ions result in a break down of the translation symmetry, leading to the failure of the zone center selection rules and a broadening of the Raman lines. On the other hand, when long-range order is achieved, zone center processes are enhanced, hence soft modes may appear at the ferroelectric phase transitions.¹² Our results show that the Pb related vibrational mode does have a noticeable change at the tetragonal to rhombohedral phase transition.

It was pointed out that the long-range order in relaxor-based ferroelectrics can be driven by either increasing the PT content or applying a dc bias.¹³ The change of dielectric constant with temperature at various frequencies is presented in Fig. 4 for both poled and depoled sample. It can be seen in the inset that the phase transition between the tetragonal and rhombohedral phases triggers a shoulder in the dielectric constant of the depoled 0.67PMN–0.33PT crystals.¹³ This transition near 70 °C becomes more evident for the poled sample as shown in Fig. 4(a), indicating that the poling process enhances the long-range order in the crystals below the Curie point. Based on this fact, we may understand our Raman data as the following.

(1) For the poled 0.67PMN–0.33PT crystal, long-range order prevails and the splitting of T_{1u} modes into A_1 and E modes occurs at the tetragonal-to-rhombohedral phase tran-

sition. Based on the crystal structure of the PMN and PT, the rhombohedral clusters represent the relaxor nature (short range order) while the tetragonal phase represents the ferroelectric nature (long range order). The new A_1 mode gives us a useful identifier for the vanishing of the long-range order when the system is transformed from tetragonal to rhombohedral phase.

(2) For the depoled sample, rhombohedral nanodomains are still present in the tetragonal phase but the cluster size becomes even smaller, which is fortunately still visible to the micro-Raman.

In conclusion, micro-Raman spectra of [001]-oriented 0.67Pb(Mg_{1/3}Nb_{2/3})O₃–0.33PbTiO₃ single crystal have been measured from –120 to 220 °C. A ferroelectric mode centered near 95 cm^{–1} at –120 °C was observed in both poled and depoled samples. For the poled sample, this mode only appears in the rhombohedral phase, hence, it can be identified as pertinent to the rhombohedral symmetry. For the depoled sample, however, this A_1 mode shifts towards the E mode while heating up toward the rhombohedral to tetragonal phase transition but never disappears or merge with the E mode. In fact, it comes back in the tetragonal phase above the rhombohedral to tetragonal phase transition temperature. The presence of the A_1 mode in the tetragonal phase in the depoled sample indicates that local clusters of rhombohedral symmetry or short-range order rhombohedral nanodomains still persist above the phase transition temperature. The long-range order, on the other hand, can be developed in the crystal through the poling process.

This research was fully supported by a grant from the Research Grants Council of the Hong Kong Special Administrative Region, China [Project No. (102104)].

¹See review article, Z. G. Ye, Key Eng. Mater. **155–156**, 81 (1998).

²S. E. Park and T. R. Shrout, J. Appl. Phys. **82**, 1804 (1997).

³R. Zhang, B. Jiang, and W. Cao, J. Appl. Phys. **90**, 3471 (2001).

⁴R. Zhang, B. Jiang, and W. Cao, Appl. Phys. Lett. **82**, 787 (2003).

⁵D. Damjanovic, M. Budimir, M. Davis, and N. Setter, Appl. Phys. Lett. **83**, 527 (2003).

⁶H. Idink and W. B. White, J. Appl. Phys. **76**, 1789 (1994).

⁷F. Jiang and S. Kojima, Jpn. J. Appl. Phys., Part 1 **38**, 5128 (1999).

⁸M. El Marssi, R. Farhi, and Y. I. Yuzyuk, J. Phys.: Condens. Matter **10**, 9161 (1998).

⁹M. Iwata, H. Hoshino, H. Orihara, H. Ohwa, N. Yasuda, and Y. Ishibashi, Jpn. J. Appl. Phys., Part 1 **39**, 5691 (2000).

¹⁰S. Kamba, E. Buixaderas, J. Petzelt, J. Fousek, J. Nosek, and P. Bridenbaugh, J. Appl. Phys. **93**, 933 (2003).

¹¹O. Svitelskiy, J. Toulouse, G. Yong, and Z. G. Ye, Phys. Rev. B **68**, 104107 (2003).

¹²A. Lebon, M. El Marssi, R. Farhi, H. Dammak, and G. Calvarin, J. Appl. Phys. **89**, 3947 (2001).

¹³J. P. Han and W. W. Cao, Phys. Rev. B **68**, 134102 (2003).

¹⁴E. Husson, L. Abello, and A. Morell, Mater. Res. Bull. **25**, 539 (1990).

¹⁵G. Burns and B. A. Scott, Phys. Rev. B **7**, 3088 (1973).

¹⁶G. Shirane, J. D. Axe, and J. Harada, Phys. Rev. B **2**, 155 (1970).

¹⁷G. Burns and F. H. Dacol, Phys. Rev. B **28**, 2527 (1983).